



UNIVERSITY OF LEEDS

This is a repository copy of *Episodic dynamic change linked to damage on the Thwaites Glacier Ice Tongue*.

White Rose Research Online URL for this paper:

<https://eprints.whiterose.ac.uk/195455/>

Version: Accepted Version

Article:

Surawy-Stepney, T, Hogg, AE orcid.org/0000-0002-6441-4937, Cornford, SL et al. (1 more author) (2023) Episodic dynamic change linked to damage on the Thwaites Glacier Ice Tongue. *Nature Geoscience*, 16. pp. 37-43. ISSN 1752-0894

<https://doi.org/10.1038/s41561-022-01097-9>

© The Author(s), under exclusive licence to Springer Nature Limited 2023. This version of the article has been accepted for publication, after peer review (when applicable) and is subject to Springer Nature's AM terms of use (<https://www.springernature.com/gp/open-research/policies/accepted-manuscript-terms>), but is not the Version of Record and does not reflect post-acceptance improvements, or any corrections. The Version of Record is available online at: <https://doi.org/10.1038/s41561-022-01097-9>.

Reuse

Items deposited in White Rose Research Online are protected by copyright, with all rights reserved unless indicated otherwise. They may be downloaded and/or printed for private study, or other acts as permitted by national copyright laws. The publisher or other rights holders may allow further reproduction and re-use of the full text version. This is indicated by the licence information on the White Rose Research Online record for the item.

Takedown

If you consider content in White Rose Research Online to be in breach of UK law, please notify us by emailing eprints@whiterose.ac.uk including the URL of the record and the reason for the withdrawal request.



eprints@whiterose.ac.uk
<https://eprints.whiterose.ac.uk/>

Episodic dynamic change linked to damage on the Thwaites Glacier Ice Tongue

Trystan Surawy-Stepney, Anna E. Hogg, Stephen L. Cornford, and Benjamin J. Davison

Abstract. The stability and dynamics of Thwaites Glacier depend on the structural properties of its marine terminus; however, the relationship between these variables on the floating ice tongue is poorly understood. Here, we present a 6-year record of ice speed, derived from satellite observations starting in 2015, showing two large-magnitude ($\sim 30\% - 45\%$) and prolonged ($\sim 1-2$ years) cycles of speed variation across the ice tongue. Using an automated, deep-learning-based method of extracting high resolution fracture maps from satellite imagery, we detail periods of increasing fracture development and subsequent reconsolidation in the ice tongue shear margin which coincide with the observed speed changes. Inverse modelling using the BISICLES ice sheet model indicates that the variation in ice speed can be accounted for by these observed changes to the spatial pattern of fracturing. This study provides further evidence of direct coupling between fracturing and dynamic variability in West Antarctica, but indicates that increased fracturing and associated speed changes are reversible on 1 to 2 year timescales. We suggest that fracturing does not necessarily lead to positive feedback with glacier acceleration on these timescales and that damage process modelling is important for accurately predicting the evolution of the Antarctic Ice Sheet.

1. Introduction

Thwaites Glacier (TG) is the largest ice stream in West Antarctica, draining a 210,600 km² catchment that holds enough ice to raise sea levels by 0.59 m alone ([1]). Satellite observations show that over the past 30-years, TG has been thinning ([2, 3]), accelerating ([4]) and retreating at the grounding line ([5]). These decadal-scale dynamic changes are thought to be driven by incursions of warm circumpolar deep water, which likely strengthened in the mid 2000's ([6–9]).

TG terminates in two distinct floating units: the Eastern Ice Shelf (EIS) and the TG Ice Tongue (TGIT). Observations show that the slower flowing EIS has weakened since the speed-up of TG intensified in ~2006 ([10]) and may be susceptible to disintegrate on a decadal timescale ([11]). The TGIT, which is, as of 2021, ~ 20 km wide, ~ 50 km long and ~ 300 m thick, is a remnant of the once much larger western ice shelf ([12]). The TGIT is heavily crevassed, is intermittently bonded to the EIS by a mixture of icebergs and sea ice, and pinned on a small bathymetric peak to the north-west (NW Pinning Point, NWPP). Historically, the TGIT has been a control on the dynamic behaviour of the EIS via the transmission of shear stress through the formerly robust eastern shear margin (ESM) ([11]). However, since the recent rapid structural weakening of the ESM and its propagation up glacier, the EIS and TGIT have largely decoupled ([4, 12]).

Ice fracture - the presence of rifts or surface/basal crevasses - is an important component of the Antarctic ice sheet system, as modifications to the stress balance caused by regions of fractured ice have a distributed effect on ice-dynamics ([13, 14]). A feedback mechanism between the acceleration of fast-flowing ice shelves in the ASE and structural deterioration of their shear margins has recently been posited ([15]). Given that the vast majority of west Antarctica's grounded ice mass loss comes from grounding line discharge ([16]), increased understanding of this potential feedback mechanism ([15]) and the wider impact of brittle processes on the stability of the region is essential for accurately predicting Antarctica's future contribution to sea level rise. However, though progress has been made ([17–22]), damage processes are not well integrated into realistic (as opposed to highly idealised) ice sheet models and large-scale quantitative observations of ice-fracture are sparse ([23]).

After a period of relatively steady flow since 2011, a ~30% increase in ice speed between late 2016 and 2017 was observed across the TGIT and the ESM ([12]). Here, we present a 6-year record of ice speed data from January 2015 to March 2021, which shows that this speed-up was the start of a period of high-magnitude (~ 30 – 45%) and short-term (~ 1 – 2 yr) episodic ice-dynamic activity on the TG ice tongue (Sect. 2). We use a deep neural network to detect surface crevassing across western TG (Sect. 2), which details the inland propagation of fractured regions of the ESM and the TGIT during each period of ice acceleration (extending observations of [12, 15]) followed by the reconsolidation of the shear margin during periods of deceleration. Numerical modelling, carried out using the BISICLES ice sheet model, indicates that the observed speed changes can be largely accounted for by the changes in structural integrity of TGIT that we observe.

2. Results

Observed Changes in Ice Speed

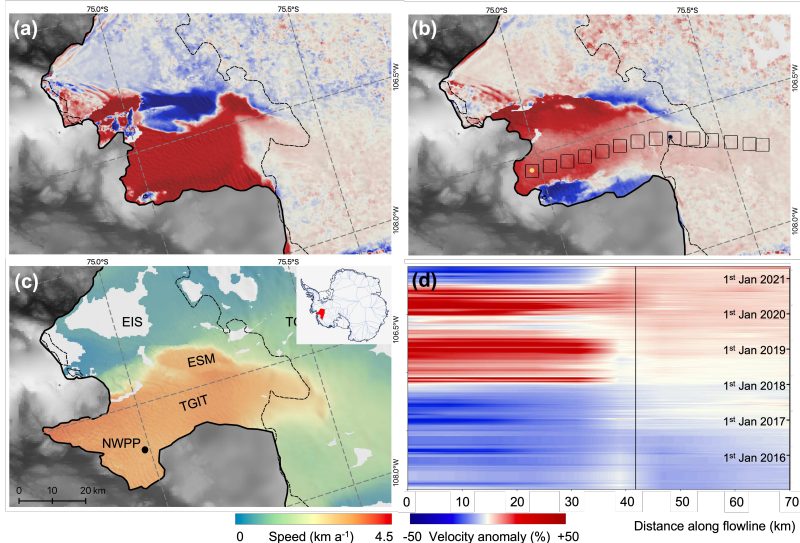


Figure 1. Ice speed anomalies Thwaites Glacier (TG). (a) Spatial pattern of ice speed anomaly observed between October 2018 and April 2019 (i.e. peak of first speed-up event) compared to the 2015-2021 mean. (b) Spatial pattern of ice speed anomaly observed between November 2019 and May 2020 (i.e. peak of second speed-up event) compared to the 2015-2021 mean. (c) Mean ice speed on TG in 2016 in kilometres per year (km a^{-1}), prior to the two ice-dynamic episodes, and locations of the Eastern Ice Shelf (EIS), the Eastern Shear Margin (ESM), the Thwaites Glacier Ice Tongue (TGIT) and the North-West Pinning Point (NWPP). (c - inset) MEaSURES grounding line, coastline and ice boundaries ([24]), with the basin and ice shelf of TG highlighted in red. Velocity data are superimposed on a 125 m resolution MODIS mosaic ([25]) and BedMachine V2 bed data ([26]) (grey shading). (d) Hovmöller diagram showing the ice speed anomaly relative to the 2015-2021 mean in a set of 14 equally spaced 4×4 km bounding boxes along a central flow-line (black box outlines Fig. 1b), with distance measured from the north (yellow point, 0 km) to the south. Linear interpolation is used in both the distance and time axes for missing data. The 2011 grounding line location is shown on Figs. 1a-c (dashed black line) and Fig. 1d (vertical black line) ([24]).

After a period of stable flow ($3.4 - 4.1 \text{ km a}^{-1}$) between 2015 and 2016, TGIT accelerated in late-June 2017, reaching peak speeds in December 2018 that were 45% ($+1.5 - 1.9 \text{ km a}^{-1}$) greater than the 2015/2016 mean (Fig. 1a). Although the 2017/18 acceleration event was extensive across the majority of the structurally weak ice tongue, we observe spatial variability in the relative speed change, with a 20 – 40% acceleration observed in the southern part of the ESM and a 20 – 60% deceleration observed on the central part

of the ESM (Fig. 1a). Between January and October 2019 the whole TGIT decelerated to its mean speed over the 2015-2021 period ($4 - 4.5 \text{ km a}^{-1}$). Whilst the TGIT decelerated, grounded ice speeds continued to steadily increase. Our observations on the TGIT show that a second speed-up event initiated in November 2019, during which the TGIT increased in speed by 25 – 30% (Fig. 1b) for a period of 6-months. In September 2020, the ice tongue decelerated back to its 2015-2021 mean speed (Fig. 1c), with a slower reduction in speed at the grounding line.

The spatial pattern of the first acceleration episode displays a well-defined boundary between the structurally weak ice tongue where a large speedup was observed, compared to the upstream region of more consolidated floating ice where ice speeds remained relatively stable (Fig. 1a). Conversely, the second acceleration episode is characterised by a softening of this boundary, with speed up observed in both regions (Fig. 1b, d), and a $\sim 6\%$ increase in speed measured at the grounding line in 2021 compared to the pre-2016 mean.

Observed Changes in Fracture

Using a deep neural network, we segment SAR backscatter images into binary maps representing observable surface fractures. These data show that between March 2016 and March 2021 there was a broad increase in the amount of severe crevassing across the surface of the TGIT (Fig. 2a-f), indicating a continued decline in its structural integrity ([12]). The deterioration of the TGIT has several key characteristics. Firstly, in the ESM and along the central portion of the TGIT we observe an overall increase in the density of crevassing throughout the study period (Fig. 2) and the upstream propagation of the region of fractured ice towards the grounding line in the central TGIT and near the ESM ([15]). Inland of the ESM, the increases in fracturing are due to new crevasses opening up in-situ, some of which caused the detachment of a $\sim 10 \text{ km}$ section of ice in March 2017 (Fig. 2b). This process also occurred on the portion of the TGIT close to the grounding line, though here, new fractures also appeared due across-flow extension of crevasses originating in the lateral margins of the TGIT (Fig. 2c-f).

The observed upstream propagation of fractured ice south of the ESM was not permanent. By March 2021, much of the fractured ice had been advected downstream, and maximum positive strain rates had decreased below the threshold required to promote the development of new crevasses (Fig. 2).

Extended Data Figure 1 shows the segmentations used in the production of Fig. ?? along with the SAR images from which the data were extracted.

Chronology of Change in Ice Speed and Structure

In order to assess the relationship between the two ice-dynamic episodes and observed changes in crevassing, we generated time-series of speed, fracture and ice shelf length on the TGIT (Fig. 3). We define “fracture density” as the fracture maps integrated over a particular region. The “relative” timeseries shown in Fig. 3c, d are created by dividing the fracture densities by the lowest value through time. The timeseries of ice shelf length was

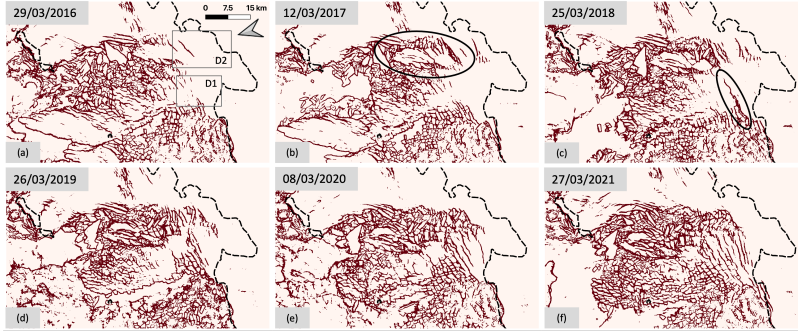


Figure 2. Observed fractures on the Thwaites Glacier Ice Tongue. Annual fracture maps generated by applying a trained neural network to Sentinel-1 SAR images acquired in March of each year during 2016 to 2021. Panels a to f show snapshots of mapped fractures (Section 2.2) on the respective dates: 29/03/2016, 12/03/2017, 25/03/2018, 26/03/2019, 08/03/2020 and 27/03/2021. Time-series of relative fracture density (Section 2.2) shown in Fig. 3c and d are extracted from bounding boxes D1 and D2. We highlight the location of a large section of ice that detached from the upstream shear margin in 2017 (black oval, Fig. 2b) and a ~ 14 km long transverse crack (black oval, Fig. 2c), with the 2011 grounding line location also shown on all maps (dashed black line) ([24]).

created using a neural network trained to segment SAR backscatter images of the TGIT into the classes “glacier” and “sea”.

Two cycles of speed change are clearly visible during the 6-year study period (Fig. 3a), characterised by two periods of elevated speed from June 2017 to April 2019 and January to September 2020, separated by a deceleration back to 2015-2021 mean speeds.

Two key structural changes on the TGIT occurred prior to the first acceleration/deceleration event. Firstly, there was a significant increase in crevassing (a factor of ~ 5 in fracture density) inland of the ESM beginning in November 2015 (D2; Fig 3d), which closely followed a loosening of the sea-ice/icebergs in the ESM ([12]). Secondly, we observed three calving events, starting in March 2016 when ~ 180 km² of ice detached from the western edge of the TGIT (Fig. 3e), in March 2017 where the northern-most 15 km of the ice tongue detached creating a ~ 235 km² iceberg ([12]), and in June 2017 where 35 km² of ice was lost (Fig. 3b, e). These latter two calving events caused the temporary unpinning of the TGIT from the NWPP for the first time on record, before it re-pinned a month later.

Following this temporary unpinning in June 2017, the first speed cycle initiated. This is characterised by a progressive increase in speed and relative fracture density until December 2018 (Fig 3). During this speed cycle, the TGIT became entirely unpinned from the NWPP in January 2018. Following this, we measured a five-fold increase in fracture density on the central trunk of TG (D1), which peaked by early November 2018 (Fig 3c), and a continued acceleration of TGIT. Crevassing inland of the ESM (D2) continued to increase until December 2018, though at a modest rate compared to that observed during 2015-2016

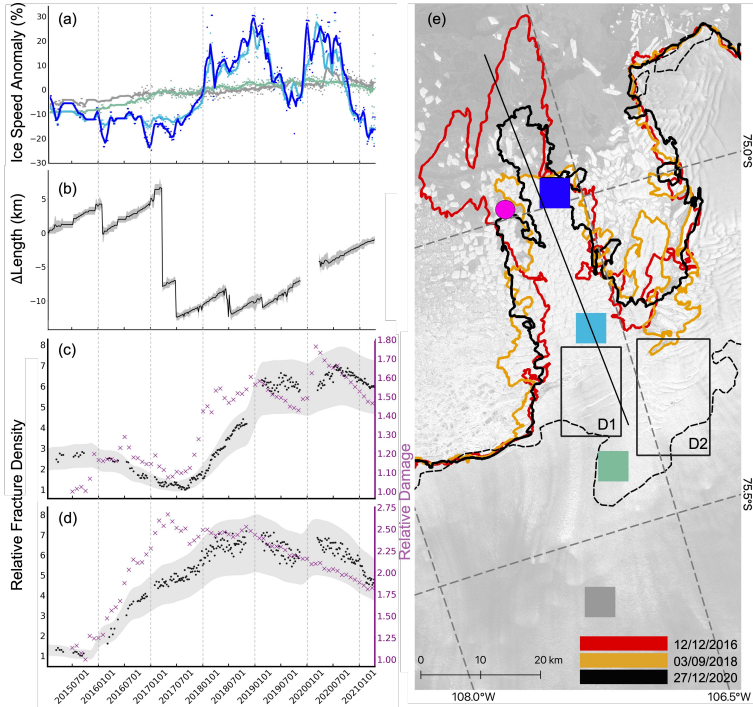


Figure 3. Time-series of Thwaites Glacier Ice Tongue (TGIT) flow and fracture. Time-series from 2015 to 2021 of: (a) the ice speed anomaly relative to the 2015–2021 mean, extracted from four 4×4 km bounding boxes along a central flow-line, where dark blue corresponds to the most seaward and grey corresponds to the most inland positions (Fig. 3e); (b) change in length of the TGIT, measured along the transect shown in (e). The uncertainty band in light-grey indicates $1-\sigma$, where σ is the width of a sigmoid-fit to the transect profile near the calving front (Supplementary Materials section 2.4.1); (c) and (d) observed fracture density (black dots) and model-inferred damage (purple crosses) extracted from bounding boxes D1 (Fig. 3c) and D2 (Fig. 3d) respectively. The uncertainty band in light grey is bounded at the top by $f \times (2 - S)$ and at the bottom by $f \times P$, where f is the fracture density and S and P are respectively the *sensitivity* and *precision* of the binary segmentations calculated from a manually annotated reference image (Supplementary Materials 2.3.1). Vertical dashed lines show the first of January of each year from 2016 to 2021. (e) Map showing the calving front location (red, orange and black lines) from 2016 to 2020 respectively on a Sentinel-1 amplitude image, the transect along which change in tongue length was calculated (straight black line), the location where velocity anomaly time-series were extracted (dark blue, light blue, turquoise and grey coloured boxes), and the locations where the fracture/damage measurements were extracted (black bounding boxes D1 and D2). The 2011 grounding line location (dashed black line) and North-West Pinning Point (NWPP) (pink dot) is also shown ([24]).

(Fig. 3d). The ice tongue grew back to within 5 km of its 2015 length (Fig. 3b), though it

did not re-pin on the NWPP. From December 2018 onwards, we observe a deceleration across the TGIT and a decrease in relative fracture density (Fig. 3). The decrease in fracture density reflects a pause in the development of new crevasses south of the ESM, and the advection of existing crevasses downstream.

Following an 8-month period of lower ice speeds ($\sim 4.5 \text{ km a}^{-1}$) from March to October 2019, we observed a more modest increase in crevassing in early 2020 on both the TGIT and ESM (Figs. 3c and 3d) which coincided with the second period of acceleration (Fig. 3a). Contact with the pinning point was remade in December 2019, though, rather than stabilising the ice tongue, this led to significant fracturing along its western edge. This re-pinning and the associated sudden structural change coincided closely with the onset of the second period of acceleration and led to a decrease in width of the TGIT (Fig. 3e), particularly at the seaward end, which was still apparent at the end of the study period in 2021.

Extended Data Figure 2 shows the segmentations used in the production of Fig. 3e along with the SAR images from which the data were extracted.

Model Inversions

We used the BISICLES ice sheet model ([27]) in combination with satellite observations to assess the link between the changing speed of the ice tongue and its local structural properties during the two major ice-dynamic episodes (Fig. 3). We do so by inferring a scalar damage parameter D (henceforth referred to as “damage”) from ice velocity observations at monthly intervals that represents an isotropic decrease in the load bearing capacity of the ice. The time-series of “relative damage” was generated by summing D over the bounding boxes (D1 and D2, Fig. 3e) and dividing by the lowest value in the timeseries. A geometrical interpretation of damage is that it represents the ratio of the vertical area of crevasses to the total area for each vertical slice, integrated over the region. This parallels our definition of observed fracture density. We assessed the quality of the model optimisation by comparing the modelled and observed velocity fields, which agreed to within $2.7 \pm 1.4\%$ on average, over the observational period.

The spatial distribution of damage and its evolution through the 6-year study period broadly resemble the observed changes in fracture at the western TG terminus (Figs. 2a-f and 3d-e). In particular, the model coarsely reproduces the observed pattern of fracture south of the ESM, with damage intensifying and propagating south-west between January 2016 and June 2019 (Fig. 4b, d), followed by the spread of severe damage north-west onto TGIT through the rest of the study period (Fig. 4d-f).

A comparison of the time-series shows that the onset and pace of change in damage exhibits significant congruity with the observed change in fracture density (Fig. 3c, d). This is especially true in D1, in which damage increases during the first acceleration event, and increases/decreases in line with fracture density thereafter, though changes appear to lead those of fracture density by 2-4 months. In D2, peak damage is reached in May 2017, prior to the start of the first period of acceleration, and two years before the maximum

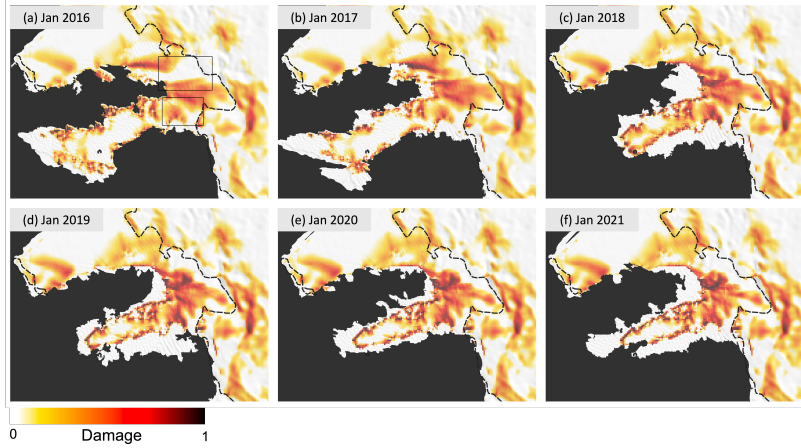


Figure 4. Annual maps of damage inferred using the BISICLES ice sheet model in January from 2016 to 2021. Panels (a) to (f) show a snapshot of damage, with the seaward limit of the model domain bounded by the observed glacier perimeter for the respective month, superimposed on a 125 m resolution MODIS mosaic ([25]). Time-series of relative damage are extracted from bounding boxes (D1 and D2, black outline) (Fig. 4a). We also highlight the location of a large section of ice that calved in 2017 (black oval, Fig. 4b), with the grounding line and pinning point locations also shown on all maps (dashed black line) ([24]).

observed fracture density, potentially indicating that fractures formed at the ice base before they manifested as surface (observable) crevasses.

3. Discussion

Long-term Context

Significant dynamic changes have occurred on TG over the last three decades, with the speed of the central trunk increasing by 50% between 1992 and 2013 ([4]), doubling TG’s sea-level contribution between 1994-6 and 2010 ([28]). Our results extend the ~ 30-year ice speed record on Thwaites Glacier to 2021, showing that the pattern of long-term speed up with 5-10 year fluctuations on the TGIT ([4, 12]), likely driven by decadal variability in ocean temperature ([9, 29]), has seen the addition of shorter-term, higher magnitude acceleration and deceleration events. This indicates that TGIT has an increasing sensitivity to external forcing and internal feed-backs. We note that historical satellite observations are of insufficient temporal resolution to resolve velocity events on annual timescales or less, therefore it is not possible to determine whether the episodic ice-dynamic behaviour that we observe is new and represents a departure from TG’s historical behaviour.

Our measurements show a detailed picture of fracturing on the ice tongue that has increased and migrated inland since 2015. Since observations of fracturing were last made on the TGIT ([12, 15]) we observe that the region south of the ESM has undergone a period of fracture development and partial re-consolidation, showing that the previously identified acceleration-damage feedback of [15] is not closed. At least, our results suggest that the ‘sign’ of the feedback reversed in the shear margin at the peak of the first speed up in December 2018, did not initiate in the second acceleration event, and did not re-emerge before the end of the observational period. This suggests a feedback that is highly sensitive to external influences. We hypothesise that the sensitivity comes from fluctuating ice thickness in the region caused by changes to basal melt rates and changing ice flux from south-east of the ESM, with thicker ice reducing the likelihood of fracturing. Though we cannot rule out the influence of other processes, such as periodic changes to the grounding line position. It is likely, therefore, that this reconsolidated section of shear margin will go through more periods of fracturing. However, our observations suggest that the decline of the TGIT via a mechanism of weakening in its shear margin and acceleration causing increased shear strain rates will not progress monotonically.

Link Between Structural Change and Dynamic Variability

At the large-scale of structural change, our observations suggest that, after acceleration and fracturing in the ESM throughout 2016, the unpinning of the TGIT from the NWPP, caused by the detachment of a large section of the ice tongue in two parts between March and June 2017, provided the conditions for the whole ice tongue to respond rapidly and dynamically to external forcing. This triggered the first acceleration event in June 2017, which was compounded by a significant decrease in the structural integrity of the ice tongue, the upstream expansion of the fractured ESM, and the propagation of damage inland along the central glacier trunk in the form of long transverse crevasses forming increasingly close to the grounding line. The weakened ice tongue was then susceptible to a further dynamic response, which manifested as the second ice-dynamic episode, where the prior inland expansion of the damaged ice likely contributed to the upstream propagation of the ice speedup and its lateral confinement to the central portion of the ice tongue. We identify the fracturing and acceleration of the ESM in 2016 to be a likely initiator of the dynamic changes seen throughout the observational period.

Previous studies have suggested that hydrofracture ([30, 31]) and unpinning ([32]) are the two primary mechanisms for ice shelf destabilisation, while other work proposes a third mechanism, termed backstress-triggered failure, where backstress from a pinning point can cause ice-shelf fragmentation ([10, 33]). Our measurements show that the fragility of the TGIT rendered it unable to form a stable configuration upon re-pinning on the NWPP in late 2019. Instead, it fractured along most of its western edge, with the affected area penetrating further into the bulk of the ice tongue as the compressive stress propagated south. This coincided with and, therefore, may have triggered the onset of the second period of acceleration in late 2019. Further studies are needed to test the impact of such a mechanism

of failure on other non-steady state ice shelf systems, as it provides a mechanism for ice shelf destabilisation in the absence of an external climatological forcing mechanism.

By showing a strong correspondence between observed fracture patterns and damage inferred by the model, we have shown that the observed dynamic changes can be accounted for with changes in the spatial distribution of damage that are comparable to the changes in fracturing that we observe. An important implication of this is that a prognostic ice sheet model without new, more sophisticated parametrisations of damage processes would not be able to simulate the behaviour of highly fractured ice-shelves. Given that forward modelling of the Antarctic Ice Sheet largely relies on fixed fields for ice rheology, and that ice shelves are of such importance to the future evolution of the ice sheet, this study demonstrates in an un-idealised setting the existence of an important missing ingredient in the simulation of future sea-level rise. We have, however, provided further evidence that the impact of real fractures on ice dynamics can be well-represented in continuum ice sheet modelling with a simple, scalar damage parameter. This provides motivation for the development of process modelling methods that treat damage as a local, isotropic change in effective ice viscosity.

While our results show that there is a continued, strong link between structural change and dynamic variability and that backstress-triggered failure likely played a causal role in the second (2020) dynamic episode, internal feedbacks cannot alone account for the initiation of the first ice-dynamic episode or the deceleration of TGIT. Instead, an external forcing mechanism is required to drive the initial damage development and calving front retreat, and, at least in part, the two deceleration events in 2019 and in the autumn of 2020 (Supplementary Material 4).

4. Conclusions

Our 6-year-long record of ice speed shows the onset and abatement of two major ice-dynamic episodes on TGIT between 2015 and 2021, which caused a 30%– ~ 45% change in ice speed relative to the 2015–21 mean over monthly to annual timescales. We developed and applied deep learning methods to map surface crevasses and calving front location on TG, and used these measurements to quantify the decrease in structural integrity of the floating ice tongue. To the best of our knowledge, this is the first automated method for the extraction of dense, high-resolution fracture time-series, and can be used for future AIS-wide analyses of the effect of damage on ice-dynamics. The fracture mapping results show that the crevassed area on the central trunk of TG expanded throughout the study period, with pronounced fracturing occurring at the time of both the first and second ice-dynamic episodes. Fracturing in the shear margin, where a positive acceleration-damage feedback has been posited, increased prior to and during the first dynamic speedup, but decreased thereafter - suggesting such a feedback has a high degree of sensitivity to external conditions. A quantitative comparison between the observed fracture and model-inferred damage indicates that the observed changes in the structural integrity of the ice tongue has played a significant role in its dynamic behaviour. The intricate coupling between ice dynamics,

calving processes, and fracture demonstrates that accurate projections of the short-term behaviour of marine terminating ice streams and their longer-term stability cannot be made without accounting for changes in the structural integrity of the ice. In the future, we must extend the observational record of ice-fracture and its change over time across the Antarctic Ice Sheet using data from both current and historical satellite missions. Ice-flow models must evolve to physically represent damage processes in forward-modelling, and must increase their capability to integrate larger volumes of observational data at fine temporal resolution in order to capture short-term behaviour.

Acknowledgments This work was led by the School of Earth and Environment at the University of Leeds. The authors would like to thank David Hogg for valuable advice regarding the deep learning methods employed in this study; Richard Rigby for advice on high-performance computing. Much of this work was undertaken on ARC4, part of the High-Performance Computing facilities at the University of Leeds, UK. The authors gratefully acknowledge ESA and the European Commission for the acquisition of Sentinel-1 data. A. E. H. and B. J. D. were supported by the NERC DeCAdeS project (NE/T012757/1) and ESA Polar+ Ice Shelves project (ESA-IPLPOE-EF-cb-LE-2019-834). S. L. C. was supported by the European Union's Horizon 2020 research and innovation programme, grant agreement no. 869304, PROTECT. We would finally like to acknowledge the anonymous referees of this article for their constructive and insightful feedback. In particular, we would like to thank the reviewer who suggested looking at the distribution of negative damage to assess the temperature component of the damage field. The LaTeX template used for this document was adapted from that of the European Mathematical Society, licenced under Creative Commons CC BY 4.0.

Authors Contributions T.S.S and A.E.H designed the work and wrote the manuscript. T.S.S processed the ice velocity observations, generated fracture maps, calving front locations and performed the analysis. T.S.S and S.C. performed the modelling and B.J.D. analysed the ocean data. All authors contributed to scientific discussion, interpretation of the results and contributed to the manuscript.

Competing Interests The authors declare no competing interests

Data Availability Ice speed data processed for and used in this study is available at: <http://www.cpom.ucl.ac.uk/csopr/iv/index.php> The BISICLES ice sheet model is publicly available at: <https://commons.lbl.gov/display/bisicles/BISICLES>. Fracture and calving front data have been submitted to PANGAEA for public access, though a DOI has not yet been provided. The data is currently available on request.

Code Availability The authors have made public a GitHub repository (<https://github.com/R-Wolfcastle/FractureS1.git>) containing a collection of python and shell scripts that can be used to make fracture maps according to the methods described in this article. Please note

that this repo is in development so specific elements like the network states and architectures are likely to be changeable.

References

- [1] J. W. Holt, D. D. Blankenship, D. L. Morse, D. A. Young, M. E. Peters, S. D. Kempf, T. G. Richter, D. G. Vaughan, and H. F. Corr, “New boundary conditions for the west antarctic ice sheet: Subglacial topography of the thwaites and smith glacier catchments,” *Geophysical Research Letters*, vol. 33, no. 9, 2006.
- [2] A. Shepherd, L. Gilbert, A. S. Muir, H. Konrad, M. McMillan, T. Slater, K. H. Briggs, A. V. Sundal, A. E. Hogg, and M. E. Engdahl, “Trends in antarctic ice sheet elevation and mass,” *Geophysical Research Letters*, vol. 46, no. 14, pp. 8174–8183, 2019.
- [3] M. McMillan, A. Shepherd, A. Sundal, K. Briggs, A. Muir, A. Ridout, A. Hogg, and D. Wingham, “Increased ice losses from antarctica detected by cryosat-2,” *Geophysical Research Letters*, vol. 41, no. 11, pp. 3899–3905, 2014.
- [4] J. Mouginot, E. Rignot, and B. Scheuchl, “Sustained increase in ice discharge from the amundsen sea embayment, west antarctica, from 1973 to 2013,” *Geophysical Research Letters*, vol. 41, no. 5, pp. 1576–1584, 2014.
- [5] P. Milillo, E. Rignot, P. Rizzoli, B. Scheuchl, J. Mouginot, J. Bueso-Bello, and P. Prats-Iraola, “Heterogeneous retreat and ice melt of thwaites glacier, west antarctica,” *Science Advances*, vol. 5, no. 1, 2019.
- [6] D. P. Walker, M. A. Brandon, A. Jenkins, J. T. Allen, J. A. Dowdeswell, and J. Evans, “Oceanic heat transport onto the amundsen sea shelf through a submarine glacial trough,” *Geophysical Research Letters*, vol. 34, no. 2, 2007.
- [7] P. Dutrieux, J. De Rydt, A. Jenkins, P. R. Holland, H. K. Ha, S. H. Lee, E. J. Steig, Q. Ding, E. P. Abrahamsen, and M. Schröder, “Strong sensitivity of pine island ice-shelf melting to climatic variability,” *Science*, vol. 343, no. 6167, pp. 174–178, 2014.
- [8] S. S. Jacobs, A. Jenkins, C. F. Giulivi, and P. Dutrieux, “Stronger ocean circulation and increased melting under pine island glacier ice shelf,” *Nature Geoscience*, vol. 4, no. 8, pp. 519–523, 2011.
- [9] P. R. Holland, T. J. Bracegirdle, P. Dutrieux, A. Jenkins, and E. J. Steig, “West antarctic ice loss influenced by internal climate variability and anthropogenic forcing,” *Nature Geoscience*, vol. 12, no. 9, pp. 718–724, 2019.
- [10] D. I. Benn, A. Luckman, J. A. Åström, A. Crawford, S. L. Cornford, S. L. Bevan, R. Gladstone, T. Zwinger, K. Alley, E. Pettit, and J. Bassis, “Rapid fragmentation of thwaites eastern ice shelf, west antarctica,” *The Cryosphere Discussions*, vol. 2021, pp. 1–25, 2021.
- [11] K. E. Alley, C. T. Wild, A. Luckman, T. A. Scambos, M. Truffer, E. C. Pettit, A. Muto, B. Wallin, M. Klinger, T. Sutterley, *et al.*, “Two decades of dynamic change and progressive destabilization on the thwaites eastern ice shelf,” *The Cryosphere Discussions*, pp. 1–31, 2021.
- [12] B. W. J. Miles, C. R. Stokes, A. Jenkins, J. R. Jordan, S. S. R. Jamieson, and G. H. Gudmundsson, “Intermittent structural weakening and acceleration of the thwaites glacier tongue between 2000 and 2018,” *Journal of Glaciology*, vol. 66, no. 257, p. 485–495, 2020.
- [13] C. P. Borstad, E. Rignot, J. Mouginot, and M. P. Schodlok, “Creep deformation and buttressing capacity of damaged ice shelves: theory and application to larsen c ice shelf,” *The Cryosphere*, vol. 7, no. 6, pp. 1931–1947, 2013.

- [14] A. Khazendar, E. Rignot, and E. Larour, “Roles of marine ice, rheology, and fracture in the flow and stability of the brunt/stancomb-wills ice shelf,” *Journal of Geophysical Research: Earth Surface*, vol. 114, no. F4, 2009.
- [15] S. Lhermitte, S. Sun, C. Shuman, B. Wouters, F. Pattyn, J. Wuite, E. Berthier, and T. Nagler, “Damage accelerates ice shelf instability and mass loss in amundsen sea embayment,” *Proceedings of the National Academy of Sciences*, vol. 117, no. 40, pp. 24735–24741, 2020.
- [16] E. Rignot, J. Mouginot, B. Scheuchl, M. van den Broeke, M. J. van Wessem, and M. Morlighem, “Four decades of antarctic ice sheet mass balance from 1979–2017,” *Proceedings of the National Academy of Sciences*, vol. 116, no. 4, pp. 1095–1103, 2019.
- [17] A. Pralong and M. Funk, “Dynamic damage model of crevasse opening and application to glacier calving,” *Journal of Geophysical Research: Solid Earth*, vol. 110, no. B1, 2005.
- [18] C. Plate, R. Müller, A. Humbert, and D. Gross, “Evaluation of the criticality of cracks in ice shelves using finite element simulations,” *The Cryosphere*, vol. 6, no. 5, pp. 973–984, 2012.
- [19] J. Åström, T. Riikilä, T. Tallinen, T. Zwinger, D. Benn, J. C. Moore, and J. Timonen, “A particle based simulation model for glacier dynamics,” *The Cryosphere*, vol. 7, no. 5, pp. 1591–1602, 2013.
- [20] J. N. Bassis and Y. Ma, “Evolution of basal crevasses links ice shelf stability to ocean forcing,” *Earth and Planetary Science Letters*, vol. 409, pp. 203–211, 2015.
- [21] S. Sun, S. L. Cornford, J. C. Moore, R. Gladstone, and L. Zhao, “Ice shelf fracture parameterization in an ice sheet model,” *The Cryosphere*, vol. 11, no. 6, pp. 2543–2554, 2017.
- [22] A. J. Crawford, D. I. Benn, J. Todd, J. A. Åström, J. N. Bassis, and T. Zwinger, “Marine ice-cliff instability modeling shows mixed-mode ice-cliff failure and yields calving rate parameterization,” *Nature communications*, vol. 12, no. 1, pp. 1–9, 2021.
- [23] C.-Y. Lai, J. Kingslake, M. G. Wearing, P.-H. C. Chen, P. Gentine, H. Li, J. J. Spergel, and J. M. van Wessem, “Vulnerability of antarctica’s ice shelves to meltwater-driven fracture,” *Nature*, vol. 584, no. 7822, pp. 574–578, 2020.
- [24] E. Rignot, J. Mouginot, and B. Scheuchl, “Measures antarctic grounding line from differential satellite radar interferometry, version 2,” 2016. Boulder, Colorado USA. NASA National Snow and Ice Data Center Distributed Active Archive Center. doi: <https://doi.org/10.5067/IKBWW4RYHF1Q>. Accessed 15/01/2021.
- [25] T. Haran, J. Bohlander, T. Scambos, T. Painter, and M. Fahnestock, “2005, updated 2013. modis mosaic of antarctica 2003-2004 (moa2004) image map, version 1. moa125_r1_hp1.img.gz,” 2013. Boulder, Colorado USA. NASA National Snow and Ice Data Center Distributed Active Archive Center. doi: <http://dx.doi.org/10.7265/N5ZK5DM5>. Accessed 14/06/2021.
- [26] M. Morlighem, E. Rignot, T. Binder, D. Blankenship, R. Drews, G. Eagles, O. Eisen, F. Ferraccioli, R. Forsberg, P. Fretwell, *et al.*, “Deep glacial troughs and stabilizing ridges unveiled beneath the margins of the antarctic ice sheet,” *Nature Geoscience*, vol. 13, no. 2, pp. 132–137, 2020.
- [27] S. L. Cornford, D. F. Martin, A. J. Payne, E. G. Ng, A. M. Le Brocq, R. M. Gladstone, T. L. Edwards, S. R. Shannon, C. Agosta, M. R. van den Broeke, *et al.*, “Century-scale simulations of the response of the west antarctic ice sheet to a warming climate,” *The Cryosphere*, vol. 9, no. 4, pp. 1579–1600, 2015.
- [28] B. Medley, I. Joughin, B. Smith, S. B. Das, E. J. Steig, H. Conway, S. Gogineni, C. Lewis, A. S. Criscitiello, J. R. McConnell, *et al.*, “Constraining the recent mass balance of pine island and thwaites glaciers, west antarctica, with airborne observations of snow accumulation,” *The Cryosphere*, vol. 8, no. 4, pp. 1375–1392, 2014.

- [29] A. Jenkins, P. Dutrieux, S. Jacobs, E. J. Steig, G. H. Gudmundsson, J. Smith, and K. J. Heywood, “Decadal ocean forcing and antarctic ice sheet response: Lessons from the amundsen sea,” *Oceanography*, vol. 29, no. 4, pp. 106–117, 2016.
- [30] T. A. Scambos, C. Hulbe, M. Fahnestock, and J. Bohlander, “The link between climate warming and break-up of ice shelves in the antarctic peninsula,” *Journal of Glaciology*, vol. 46, no. 154, p. 516–530, 2000.
- [31] T. Scambos, C. Hulbe, and M. Fahnestock, “Climate-induced ice shelf disintegration in the antarctic peninsula,” *Antarctic Peninsula Climate Variability: Historical and Paleoenvironmental Perspectives*, *Antarct. Res. Ser.*, vol. 79, pp. 79–92, 2003.
- [32] P. Holland, A. Brisbourne, H. Corr, D. Mcgrath, K. Purdon, J. Paden, H. Fricker, F. Paolo, and A. Fleming, “Oceanic and atmospheric forcing of larsen c ice-shelf thinning,” *The Cryosphere*, vol. 9, no. 3, pp. 1005–1024, 2015.
- [33] D. G. Vaughan, “Implications of the break-up of wordie ice shelf, antarctica for sea level,” *Antarctic Science*, vol. 5, no. 4, p. 403–408, 1993.

Trystan Surawy-Stepney

School of Earth and Environment, University of Leeds, Leeds, United Kingdom;
t.surawystepney@leeds.ac.uk

Stephen L. Cornford

School of Geographical Sciences, University of Bristol, Bristol, United Kingdom;

Anna E. Hogg

School of Earth and Environment, University of Leeds, Leeds, United Kingdom;

Benjamin J. Davison

School of Earth and Environment, University of Leeds, Leeds, United Kingdom;